

Spatiotemporal Variation of Trace Elements and Stable Isotopes in Subtropical Estuaries: II. Regional, Local, and Seasonal Salinity-Element Relationships

John A. Mohan · Benjamin D. Walther

Received: 19 February 2014 / Revised: 25 August 2014 / Accepted: 25 August 2014 / Published online: 18 September 2014
© Coastal and Estuarine Research Federation 2014

Abstract Trace elements and stable isotopes are commonly used in chronologically formed biominerals as proxies of temperature and/or salinity in estuarine and marine environments. To accurately use the chemistry of biominerals as salinity proxies, understanding the consistency of dissolved element-salinity relationships across spatiotemporal scales is essential. We examined relationships between dissolved Ba:Ca, Sr:Ca, Mg:Ca, Mn:Ca, $\delta^{18}\text{O}$, and salinity on regional, local, and seasonal scales in the lower portions of subtropical estuaries (salinities 15–42 ppt) of Texas, including locations where seasonal alternations between negative and positive estuaries can occur. Across all spatiotemporal scales, Ba:Ca displayed a negative linear relationship within the sampled salinity range and was elevated at sites furthest from the ocean and lowest at locations closest to the Gulf of Mexico. This pattern remained consistent as the neutral estuary switched from negative to positive after a rain event. On regional scales, $\delta^{18}\text{O}$ displayed a positive linear relationship with salinity and was strongly related to evaporation rates. On local and seasonal scales, evaporation-enriched $\delta^{18}\text{O}$ at upper enclosed estuarine sites and this pattern was consistent over time including periods of reverse estuary conditions. Dissolved Sr:Ca and Mg:Ca varied linearly with salinity on regional scales but displayed minimal variation across temporal scales within an estuary. High variability in dissolved Mn:Ca-salinity relations was found at all spatiotemporal scales, with localized episodic peaks of Mn:Ca possibly due to sediment disturbance. Although dissolved Ba:Ca and $\delta^{18}\text{O}$ were not predictably related to salinity

on local scales, consistent up-estuary enrichment and lower-estuary depletion make these two constituents reliable proxies for animal movements across the ocean–estuary gradient as recorded in chronologically formed biominerals.

Keywords Trace elements · Stable oxygen isotopes · Salinity · Hypersalinity · Subtropical

Introduction

The physicochemical properties of estuaries are often highly dynamic and can exhibit considerable temporal and spatial variation. The mixing of fresh river water and seawater results in gradients of salinity, ionic strength, pH, dissolved organic carbon (DOC), nutrient concentrations, and alkalinity, all which influence the distribution and behavior of many trace elements and isotope ratios (Benoit et al. 1994; Fry 2002). The concentrations of many trace elements in freshwater end-members are controlled by the weathering of terrigenous minerals with rock composition and age influencing element type and abundance (Middelburg et al. 1988; Negrel et al. 1993). In the estuarine mixing zone, sorption–desorption processes may alter the concentrations of certain elements. Removal processes of trace elements include complexation of metals with organic ligands (Wen et al. 1999), while sediment resuspension due to tidal action, storms, or biological activity may supply elements to either dissolved or particulate pools (Zhang 1995; Zwolsman and van Eck 1999). While some elements display conservative behavior across salinity gradients with linear salinity-element relationships that result from simple dilution between two end-members (Fry 2002), non-conservative (non-linear) salinity-element relationships may occur if estuarine mixing is influenced by a third end-member or by biogeochemical processes and/or anthropogenic activities (Paucot and Wollast 1997) that supply or remove

Communicated by Dennis Swaney

Electronic supplementary material The online version of this article (doi:10.1007/s12237-014-9876-4) contains supplementary material, which is available to authorized users.

J. A. Mohan (✉) · B. D. Walther
Marine Science Institute, The University of Texas at Austin, 750
Channel View Drive, Port Aransas, TX 78373, USA
e-mail: john.mohan@utexas.edu

dissolved constituents resulting in uncoupling of predictive relationships to salinity (Morris et al. 1978).

Salinity-constituent relationships have been examined in several estuarine systems, and the behavior of individual constituents depends strongly on the degree to which additions, removals, or isotopic fractionation alters constituent values across the estuarine gradient. Strontium, magnesium, and calcium often exhibit conservative behavior and increase linearly with salinity in most estuaries (Dorval et al. 2005; Gillanders and Munro 2012); however, exceptions do occur where freshwater end-members (i.e., strontium) may be higher in freshwater compared to marine end-members (Kraus and Secor 2004). Curvilinear behavior for these constituents may also result when, for instance, groundwater addition introduces a third end-member at intermediate salinities (Walther and Nims 2014). Dissolved barium typically displays non-conservative behavior with high concentrations at low salinities due to desorption from suspended particulate matter in the estuarine mixing zone, normally followed by linear mixing with salinity for the remainder of the gradient (Hanor and Chan 1977; Coffey et al. 1997). Manganese is redox-sensitive and the dissolved species (Mn^{2+}) shows high variability due to release from sediment reduction of organic matter in suboxic and anoxic conditions and vertical supply to the water column (Trefry and Presley 1982; Klinkhammer and McManus 2001). Decreases in pH and physical disturbances of the sediments affect release of Mn to a much greater degree than changes in dissolved oxygen or salinity (Atkinson et al. 2007), and this sensitivity to environmental parameters often leads to high seasonal and spatial variability in concentrations (Shiller 1997; Dorval et al. 2005; Kowalski et al. 2012). Finally, $\delta^{18}\text{O}$ -stable isotope values in estuarine waters are influenced by fractionation associated with precipitation and evaporation processes as well as the composition of the freshwater end-member and often show strong linear relationships with salinity (Ingram et al. 1996; Cooper et al. 1997).

Estuary-to-ocean salinity gradients in subtropical Texas estuaries can fluctuate temporally due to seasonal differences in freshwater inputs associated with precipitation events (Flint 1985; Nielsen-Gammon et al. 2005). On a large spatial scale, the coast of Texas displays a north–south latitudinal climatic and hydrologic gradient. Increased rainfall and freshwater inflow occur in the northern estuaries, while southern estuaries experience half the amount rainfall and orders of magnitude less freshwater inflow compared to northern estuaries (Tolan 2007). Salinity regimes of estuaries along the north–south Texas coast are characterized as positive, neutral, and negative. North Texas estuaries receive consistent rainfall and fluvial freshwater inputs and thus remain positive year-round, while in south Texas estuaries, evaporation greatly exceeds freshwater inputs resulting in hypersaline conditions and negative estuaries, such as the Laguna Madre (Tolan 2007). Central Texas estuaries, such as the Mission-Aransas, can alternate between positive and

negative regimes throughout the year due to seasonal precipitation events and can be considered neutral estuaries (Tolan 2007).

Hypersaline conditions (salinity >35 ppt) and reverse estuary behavior can potentially disrupt expected constituent-salinity relationships. For instance, Gillanders and Munro (2012) reported that dissolved barium concentrations within the Australian Coorong Lagoon decreased from freshwater to marine salinities and then dramatically increased in hypersaline waters with salinities above 40 ppt, a previously undocumented phenomenon. Therefore, more studies on constituent-salinity relationships in hypersaline conditions are necessary, especially for dissolved elements that are typically used in biogenic calcified structures as salinity proxies (Diouf et al. 2006; Gillanders and Munro 2012). If linear behavior was disrupted due to hypersalinity, then predictive relationships of dissolved elements to salinity would not hold, leading to inaccurate interpretations of salinity proxies, such as the calcified earstones of fish (otoliths) which are commonly used to estimate migratory fish movement across salinity gradients.

In this study, we investigated the consistency of element-salinity relationships across local, regional, and seasonal scales in subtropical Texas estuaries. This study examined constituent-salinity relationships in three contexts. First, relationships were evaluated across three separate estuaries across the entire Texas coast, including a positive, neutral, and negative estuary to determine regional patterns. Second, relationships were evaluated within each of the three estuary types to determine local patterns. Third, constituents were monitored within the neutral estuary at several fixed stations over a span of 12 months to determine seasonal patterns. Over the duration of the 12-month study, the salinity regime in the neutral estuary reversed from a negative to a positive regime after heavy spring precipitation, allowing us to examine the consistency of element-salinity relationships after an elevated freshwater inflow period. In the neutral estuary, environmental and climatic time series were examined for correlations to dissolved elemental and isotopic constituents to explore possible mechanisms driving the observed seasonal patterns. This project focused on relationships observed for the lower estuarine regions with salinities >15 ppt given that the dynamics of the freshwater end-members are addressed in a companion paper (Walther and Nims 2014).

Materials and Methods

Study Area and Environmental Data

To examine coast-wide geographic variation in dissolved chemistry, replicate samples were collected from five sites within Galveston Bay (GB, a positive estuary), the Mission-

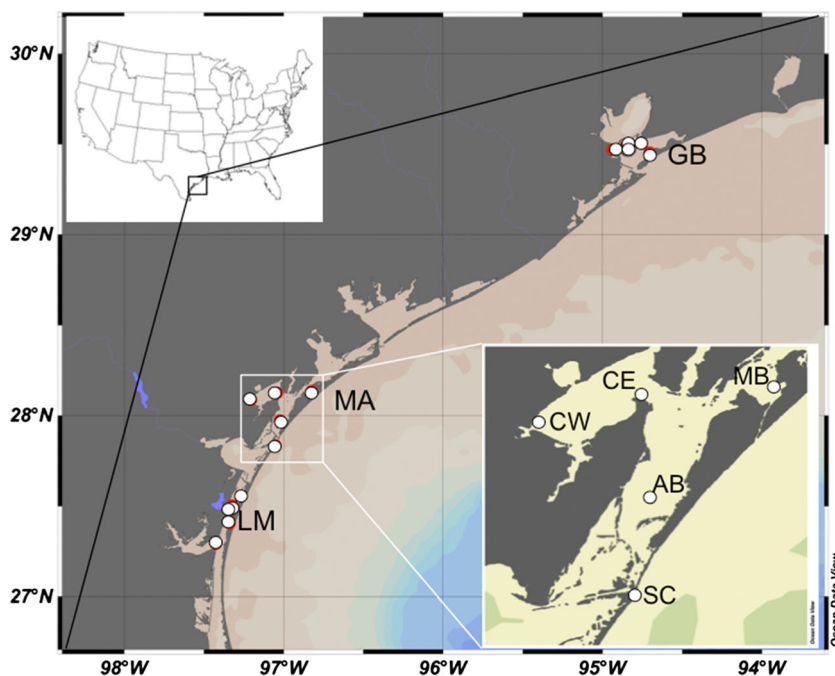
Aransas estuary (MA, a neutral estuary), and the Laguna Madre (LM, a negative estuary; Fig. 1). Each estuary was sampled in July 2012 within ten consecutive days to reduce temporal variation and make spatial comparisons between estuaries. To assess temporal variation across the seasons, the Mission-Aransas estuary was sampled monthly from October 2011 through September 2012 at five fixed stations that form the Mission-Aransas National Estuarine Research Reserve System Wide Monitoring Program (MANERR SWMP; Fig. 1). At each station, a YSI 600XL sonde measured temperature, salinity, dissolved oxygen, and pH, and water samples were collected for trace elements and isotopes as described below. The environmental parameters were measured to investigate alternative (i.e., other than salinity) influences on element behavior. For example, phytoplankton may influence dissolved element behavior through biological uptake or absorption/desorption processes (Stecher and Kogut 1999). Chlorophyll *a* samples were passed through Whatman GF/F filters and extracted with 90 % acetone, and concentrations were determined using a Turner Designs Trilogy Fluorometer as described by Mooney and McClelland (2012). Daily cumulative precipitation data recorded at the Copano East (CE) site were downloaded from the NOAA NERR Centralized Data Management Office website <http://cdmo.baruch.sc.edu> on August 6, 2013. Mean monthly precipitation values were calculated from these data for graphical display. Mean monthly discharge data was downloaded from U.S. Geological Survey website <http://waterdata.usgs.gov/nwis> for gauge station 8189500 in Refugio, TX on the Mission River that drains into Copano

Bay, for gauge station 8188500 in the San Antonio River, and gauge 8176500 in the Guadalupe River. These three river gauge stations were selected as they characterize the dominant contributors to water inflow in the Mission-Aransas estuary from the north (Mission River) and the east (San Antonio and Guadalupe Rivers) (Ward 2010). Mean monthly lake evaporation data was downloaded from the Texas Water Development Board website (<http://www.twdb.texas.gov/surfacewater/conditions/evaporation/index.asp>) from indexed regions 813 (Galveston Bay), 910 (Mission-Aransas), and 1010 (Laguna Madre). Mean monthly evaporation rates were compared between the three regions from September 2011 through October 2012. July 2012 evaporation rates were then plotted against regional mean $\delta^{18}\text{O}$ values in July.

Water Sample Collection

Surface water samples were obtained using a portable sampler (Barnant Company) equipped with a peristaltic pump (Masterflex Easy Load L/S, Cole Parmer) and acid-washed tubing (Masterflex C-Flex L/S 17) deployed at approximately 0.5 m depth from the leeward side of a small fiberglass boat. Sample water was collected in 30-ml acid-washed polytetrafluorethylene (PTFE) syringes (Norm-Ject) that were rinsed with three sample volumes before being filtered into 30-ml acid-washed LDPE Nalgene bottles with acid-washed 0.45- and 0.2- μm PTFE filters (Sartorius Stedim Minisart SRP 25). Filtered water was fixed to pH <2 with trace metal grade nitric acid (Aristar Ultra) and refrigerated until analysis.

Fig. 1 Map of water sampling locations (white dots) in Galveston Bay (GB), Mission-Aransas (MA), and Laguna Madre (LM). Five fixed stations Copano West (CW), Copano East (CE), Mesquite Bay (MB), Aransas Bay (AB), and Ship Channel (SC) were sampled monthly in Mission-Aransas



Oxygenstable isotope samples were syringe filtered (0.45 and 0.2 μm) into 30-ml amber glass vials (Fisherbrand) that were filled to overflowing to eliminate headspace and refrigerated until analysis. Ultrapure (18.2 M Ω cm) water was filtered in the field as described above to serve as method blanks during laboratory analysis.

Water Sample Analysis

All samples were analyzed at the University of Texas Jackson School of Geosciences. Trace elements ^{24}Mg , ^{40}Ca , ^{55}Mn , ^{88}Sr , and ^{137}Ba were quantified using an Agilent 7500ce quadrupole inductively coupled plasma mass spectrometer (ICP-MS) run in solution mode. Samples were diluted 100 \times by weight using 2 % ultrapure trace metal grade nitric acid. A subset ($N=12$) of samples were spiked with an internal multi-element standard solution to assess mean spike recoveries (mean 98 %) and monitor instrument drift. An external standard reference material NIST 1643e diluted 10 \times was used to determine accuracy and was between 5 and 10 % for all elements. Elemental counts were converted to concentrations using internally spiked standards and then converted to molar element:Ca ratios. Stable oxygen isotopes were analyzed with a Thermo Electron 253 isotope ratio mass spectrometer (IRMS) coupled to a Gasbench II. One milliliter of sample water was equilibrated with 3,000 ppmV CO_2 in helium for 24 h at 25 $^\circ\text{C}$, and the equilibrated headspace CO_2 was sampled in continuous flow. Laboratory standards were calibrated against Vienna Standard Mean Ocean Water (VSMOW), and reported $\delta^{18}\text{O}$ values were reproducible within 0.05 ‰. Linear regression was used to investigate the strength of element-salinity relationships against the null hypothesis that the slope=0 at regional, local, and seasonal scales. Local salinity-element regressions within a particular estuary represent small-scale mixing and dilution processes, which are different mechanisms compared to regional regressions, which depict larger-scale climatic controls, such as temperature, inflow, and evaporation. Regional lake evaporation data from July was plotted against $\delta^{18}\text{O}$ values to examine relationships. For the Mission-Aransas annual dataset, Pearson correlations were compared between dissolved elements and physicochemical parameters (salinity, temperature, DO, Chl *a*) to investigate potential relationships. Evaporation rate data was excluded from the correlation analysis because only a single regional value was available and not site-specific indices. The ship channel (SC) site was excluded from correlation analysis because it is primarily oceanic Gulf of Mexico water (Fig. 1) and was missing data for January and February. Values of pH

were missing from several sites and months and so were also excluded from correlation analysis.

Results

Regional Relationships

Water samples across all estuaries and locations sampled in July 2012 included salinities ranging from 15.7 to 43.8 ppt. Within each estuary, salinity ranges were 15.7–22.4 (Galveston Bay), 29–36.4 (Mission-Aransas), and 42.2–43.8 (Laguna Madre). For the regional scale comparison of constituents across all three estuaries, all element-salinity relationships were statistically significant and positive, except for expected negative relationship for Ba:Ca (Table 1 and Fig. 2). Barium:Ca displayed the highest range in observed values across the salinity gradient, ranging from 5 to 150 $\mu\text{mol/mol}$, with a slope of -3.21 ± 0.6 and an intercept of 175 ± 21 $\mu\text{mol/mol}$ (Table 1). The elemental ratios Sr:Ca and Mg:Ca exhibited minimal variation across the salinity range (~ 1 mmol/mol) but were strongly related to salinity and had similar slopes of approximately 0.03 (Table 1). Values of $\delta^{18}\text{O}$ ranged from -0.3‰ in Galveston Bay to 2.5 ‰ in Laguna Madre with a slope of 0.1 ± 0.008 (Table 1). Notably, $\delta^{18}\text{O}$ values were most enriched at the southern Laguna Madre sampling sites, moderately enriched at Mission-Aransas, and closer to typical Gulf of Mexico values ($\sim 0\text{‰}$) in the northern Galveston Bay, corresponding to the average salinity ranges encountered during sampling within each estuary and regional evaporation rates in July (Fig. 3). Manganese:Ca showed high variability even within replicate samples, resulting in large error bars, but still displayed a significant positive relationship to salinity (Fig. 2).

Local Relationships

Examining relationships on a local scale within each estuary, fewer elements displayed statistically significant linear relationships, likely due to restricted salinity ranges observed in each of the estuaries (Fig. 2). No significant relationships were detected in Laguna Madre, which was not surprising given that salinities only ranged from 42.2 to 43.8 ppt. Barium:Ca was significantly negatively related to salinity in both Galveston Bay (slope= -9.7 ± 2.6 ; intercept= 294 ± 50) and Mission-Aransas (slope= -12.2 ± 1.9 ; intercept= 454 ± 61 $\mu\text{mol/mol}$) (Table 1 and Fig. 2). Strontium:Ca was not significantly related to salinity within any estuary; however, Mg:Ca was significantly related to salinity in GB with a very similar slope and intercept compared to the regional regression (Table 1). Values of $\delta^{18}\text{O}$ displayed a negative statistically significant relationship to salinity in Mission-Aransas;

Table 1 Linear relationships between salinity and dissolved elemental and isotopic constituents at regional, local, and seasonal scales. Slope and intercept estimates are presented \pm SE. Only statistically significant relationships testing the null hypotheses that slope=0 are reported

Scale	Bay	Site	Element	Equation	r^2	F	p
Regional	All	All	Sr:Ca mmol/mol	$Y=0.033\pm 0.003\times X+6.99\pm 0.09$	0.83	136.6	<0.0001
	All	All	Ba:Ca μ mol/mol	$Y=-3.21\pm 0.6\times X+175\pm 21$	0.65	24.67	0.0003
	All	All	Mg:Ca mol/mol	$Y=0.028\pm 0.002\times X+3.92\pm 0.07$	0.91	147.6	<0.0001
	All	All	Mn:Ca μ mol/mol	$Y=0.25\pm 0.05\times X-4.63\pm 1.7$	0.64	23.42	0.0003
	All	All	$\delta^{18}\text{O}$ per mil	$Y=0.10\pm 0.008\times X-1.94\pm 0.3$	0.85	160.7	<0.0001
Local	GB	All	Ba:Ca μ mol/mol	$Y=-9.77\pm 2.6\times X+294\pm 50$	0.63	13.89	0.0058
	GB	All	Mg:Ca mol/mol	$Y=0.038\pm 0.01\times X+3.73\pm 0.2$	0.54	9.37	0.0156
	GB	All	Mn:Ca μ mol/mol	$Y=-0.0037\pm 0.0005\times X+0.16\pm 0.01$	0.85	47.14	0.0001
Local	MA	All	Ba:Ca μ mol/mol	$Y=-12.2\pm 1.9\times X+454\pm 61$	0.83	39.36	0.0002
	MA	All	Mn:Ca μ mol/mol	$Y=1.05\pm 0.3\times X-29.21\pm 8.5$	0.65	15.04	0.0047
	MA	All	$\delta^{18}\text{O}$ per mil	$Y=-0.093\pm 0.02\times X+4.34\pm 0.7$	0.67	16.54	0.0036
Seasonal	MA	All	Ba:Ca μ mol/mol	$Y=-4.60\pm 1.1\times X+211\pm 36$	0.27	18.77	<0.0001
	MA	All	$\delta^{18}\text{O}$ per mil	$Y=0.065\pm 0.02\times X-0.72\pm 0.7$	0.18	11.13	0.0016
Seasonal	MA	CW	Ba:Ca μ mol/mol	$Y=-6.46\pm 2.5\times X+307\pm 84$	0.42	6.51	0.0311
	MA	CW	$\delta^{18}\text{O}$ per mil	$Y=0.090\pm 0.03\times X-0.81\pm 0.9$	0.55	10.93	0.0091
Seasonal	MA	CE	$\delta^{18}\text{O}$ per mil	$Y=0.099\pm 0.02\times X-1.56\pm 0.6$	0.77	29.31	0.0004
Seasonal	MA	MB	Ba:Ca μ mol/mol	$Y=-2.70\pm 1.1\times X+145\pm 35$	0.42	6.453	0.0317
	MA	MB	Mn:Ca μ mol/mol	$Y=0.44\pm 0.09\times X-8.46\pm 10$	0.74	26.15	0.0006
	MA	MB	$\delta^{18}\text{O}$ per mil	$Y=0.076\pm 0.02\times X-1.19\pm 0.6$	0.64	15.91	0.0032
Seasonal	MA	AB	$\delta^{18}\text{O}$ per mil	$Y=0.11\pm 0.03\times X-2.56\pm 1.1$	0.58	12.52	0.0063
Seasonal	MA	SC	$\delta^{18}\text{O}$ per mil	$Y=0.11\pm 0.03\times X-3.27\pm 1$	0.69	15.83	0.0053

however, the negative relationship was driven by local evaporation and not salinity and thus the regression line is not plotted (Fig. 2). Significant relationships between Mn:Ca and salinity were negative in Galveston Bay and positive in Mission-Aransas (Table 1). Overall, the Mn:Ca-salinity regression parameters of slope and intercept were highly variable with large errors (SE) when comparing local to region regressions and even local to local (Galveston Bay and Mission-Aransas) regressions (Table 1).

Seasonal Relationships

Mean lake evaporation rates increased threefold from winter to summer, and regional evaporation rates consistently ranked Laguna Madre > Mission-Aransas > Galveston Bay during the summer (Fig. 3). From October to April, the Mission-Aransas was a negative estuary with higher salinities at Copano West, the site farthest inland from the ocean (Figs. 1 and 4). Local precipitation gradually increased in the winter, after which a large rain event in April resulted in a 20-fold increase in Mission River discharge into Copano Bay (Fig. 5). Additionally, the combined flow of the San Antonio and Guadalupe Rivers also peaked in February and March (Fig. 5). The earlier peak in flow from the San Antonio and Guadalupe Rivers was expected given their sensitivity to

rainfall events across the entire watersheds that span significant portions of Texas. This punctuated rainfall and subsequent inflow effectively reversed Mission-Aransas back to a positive estuary from April through September (Fig. 4). Geographic differences in the influence of specific tributaries on salinity at certain sites were evident. For instance, salinity at the Mesquite Bay site began to decline in March concurrent with elevated inflow from the San Antonio and Guadalupe Rivers, whereas salinity at Copano East declined in April–May after the April peak in inflow from the Mission River. These patterns were expected given the close proximities of the Mesquite Bay and Copano East sites to the mouths of the Guadalupe or Mission river mouths, respectively. The elevated springtime discharge also increased pH from May to June at all sites except Ship Channel (Fig. 4). All sites had similar temperatures each month, with January exhibiting the lowest temperature of 15 °C that increased each month until reaching a plateau in the summer at 29 °C (Fig. 4). Dissolved oxygen was highest in December and gradually declined into the summer as temperatures increased (Fig. 4). Chlorophyll *a* displayed peaks in the following months and locations: January in Copano West; January and March in Copano East; December and March in Mesquite Bay; and April in all sites except Mesquite Bay. In May, Chl *a* decreased at all sites and remained low throughout the

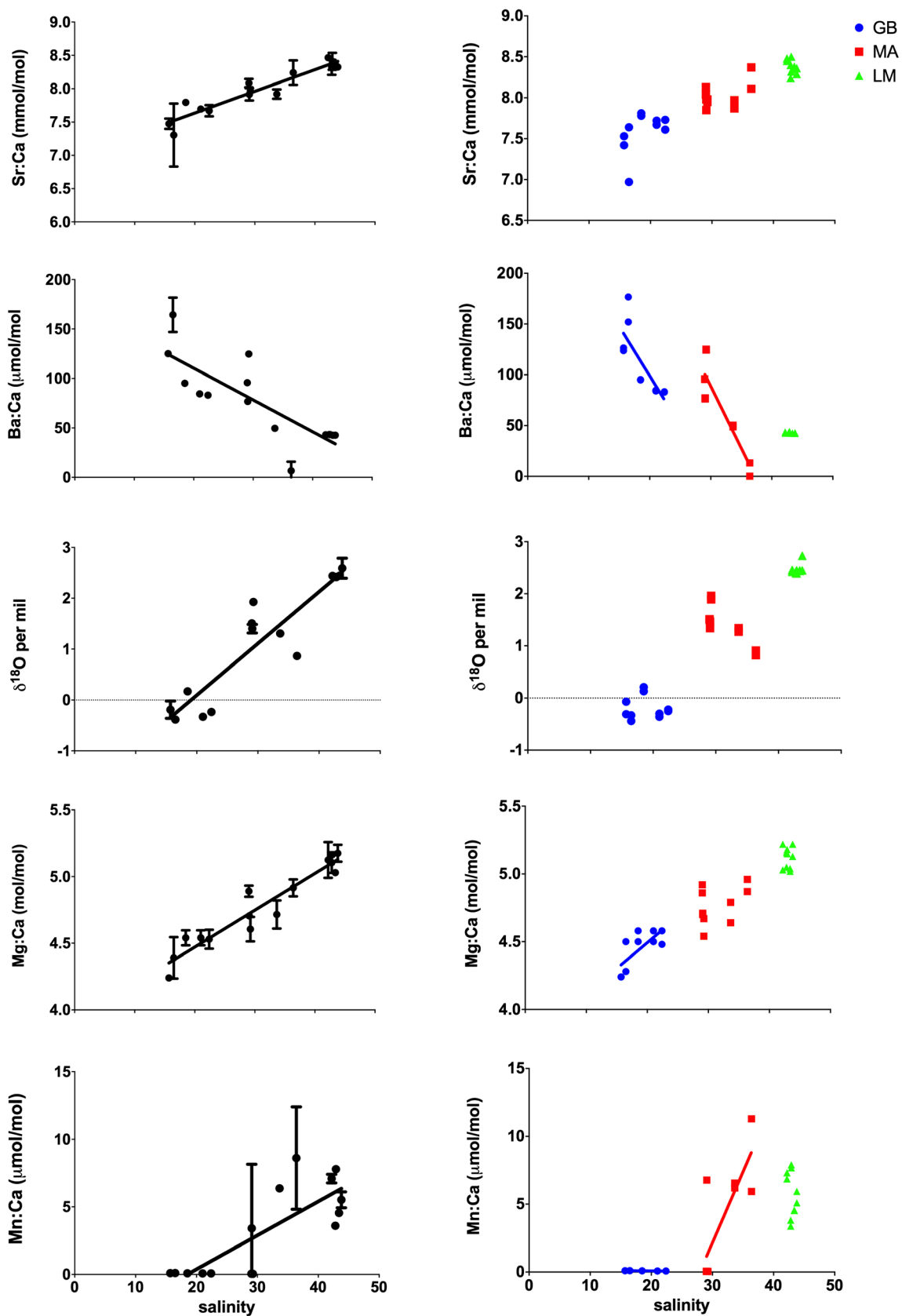


Fig. 2 Element-salinity relationships on regional (*left column*) and local (*right column*) scales from samples collected in July 2012. Plotted lines display significant linear regressions (excluding $\delta^{18}\text{O}$ in Mission-

Aransas). Error bars indicate standard deviation from two replicate samples for regional data. Dotted lines indicate expected oceanic $\delta^{18}\text{O}$ value of 0‰

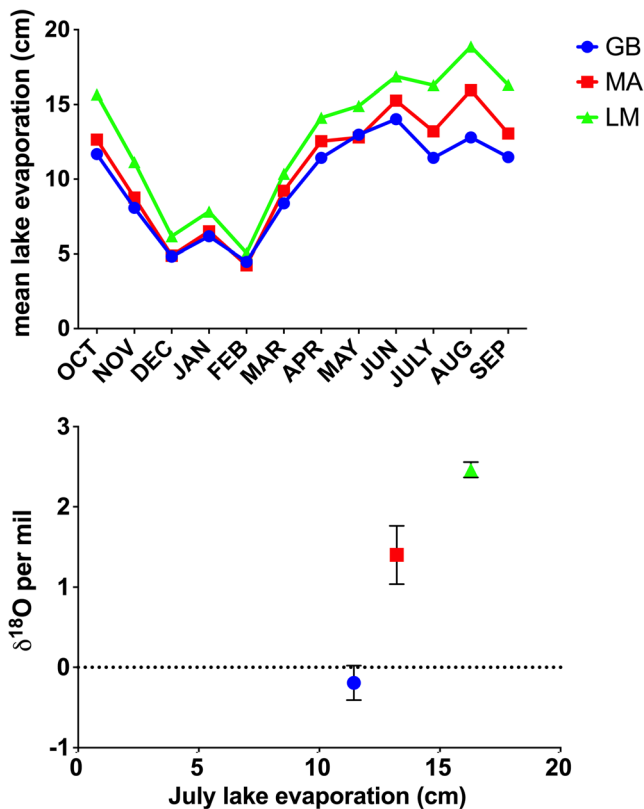


Fig. 3 Mean monthly lake evaporation rates for Galveston Bay (GB), Mission-Aransas (MA), and Laguna Madre (LM) and relationship to mean July $\delta^{18}\text{O}$ in each bay

summer and fall compared to the winter and spring (Fig. 4).

Values of Ba:Ca showed a consistent up-estuary to ocean gradient, with rankings in Ba:Ca values of Copano West > Copano East > Mesquite Bay > Aransas Bay > Ship Channel during all months of the year except January and February, when a distinct drop in values occurred at all sites (Fig. 6). Values of $\delta^{18}\text{O}$ were enriched above typical oceanic values and displayed an up-estuary to ocean gradient for all months except during May when values converged following the discharge event (Fig. 6). Strontium:Ca, Mg:Ca, and Mn:Ca exhibited limited variation throughout the year, except for a large spike in Mn:Ca in January at Copano East (Fig. 6). Seasonal consistency of element-salinity relationships was investigated by using linear regression analysis on the year-long Mission-Aransas data set for all sites together and then for each site individually. For all sites combined across the year, Ba:Ca was negatively related to salinity and $\delta^{18}\text{O}$ was positively related to salinity, and the regression parameters (slope and intercept) were very similar to the regional regressions (Table 1 and Fig. 7). Similarly, $\delta^{18}\text{O}$ was significantly positively related to salinity within each individual bay throughout the year, while Ba:Ca was significantly negatively related to salinity in Copano West and Mesquite Bay across

the seasons (Table 1 and Fig. 7). However, a single January data point largely drove the regression in Copano West and the relationship became insignificant if the January point was removed ($F=1.15$; $p=0.319$). The Ba:Ca-salinity relationship in Mesquite Bay became stronger with the r^2 increasing to 0.65 if the January data point was removed. Although there was a significant relationship found between Mn:Ca and salinity in Mesquite Bay, the regression parameters were inconsistent when compared to regional and local regressions (Table 1 and Fig. 7).

Correlation analysis revealed that Ba:Ca was negatively correlated to salinity and positively correlated to temperature (Table 2). Oxygen-stable isotopes were positively correlated to salinity, but no other elements displayed significant correlations to salinity, temperature, DO, or Chl *a* (Table 2).

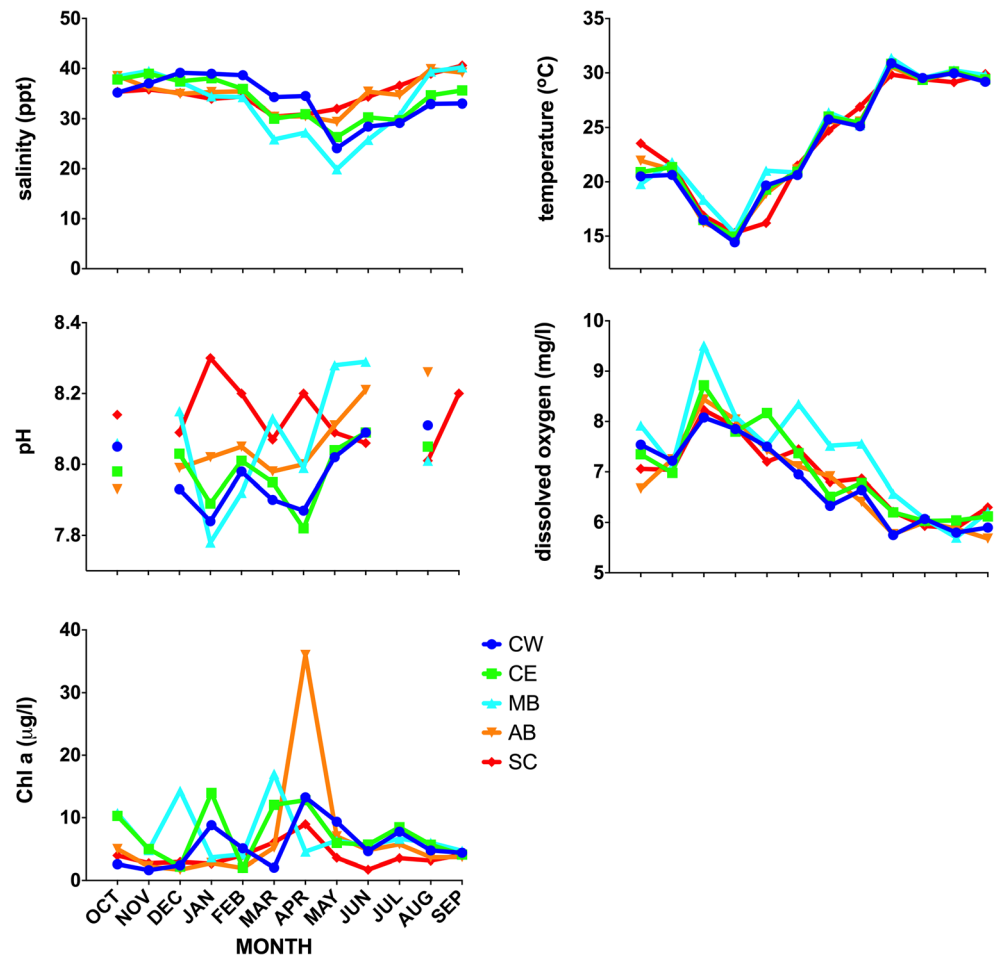
Discussion

Across the Texas coast, constituent-salinity regressions were significant and linear for dissolved Ba:Ca, Sr:Ca, Mg:Ca, Mn:Ca, and $\delta^{18}\text{O}$ across large spatial scales. For these comparisons, salinity was considered a proxy for regional differences in climate and the balance between evaporation and inflow, rather than representing a mixing relationship between fresh and marine end-members as would occur within a given estuary. On finer local scales within individual estuaries and on temporal scales of 1 year, Ba:Ca and $\delta^{18}\text{O}$ displayed consistent up-estuary to down-estuary gradients, even though the Mission-Aransas estuary reversed from negative to positive after a rain event, uncoupling the direct relationship of Ba:Ca to salinity. Dissolved elements that display consistent up-estuary enrichment and lower-estuary depletion are reliable candidates for studying animal movements across the ocean-estuary gradient, by quantifying elemental changes in chronologically formed binomials.

Spatial Patterns

In our study, dissolved Ba:Ca demonstrated the most consistent linear behavior across all scales of space and time over the salinity range sampled. Slopes of the Ba:Ca-salinity relationship were similar on regional ($b=-3.2$) and seasonal ($b=-4.6$) scales but slightly higher on local ($b_{\text{GB}}=-9.8$; $b_{\text{MA}}=-12.2$) scales. In the Mission-Aransas Estuary, only the Copano West and Mesquite Bay sites maintained significant Ba:Ca-salinity regressions on seasonal scales, possibly due the influence of the Mission River inflows on Copano West and the influence of the combined San Antonio plus Guadalupe River inflows on Mesquite Bay. The Mission-Aransas Ba:Ca-salinity relationship displayed the largest y-intercept (454 $\mu\text{mol/mol}$), which is within error of the mean freshwater end-member

Fig. 4 Time series of physicochemical parameters and Chl *a* concentrations from October 2011 to September 2012 in the Mission-Aransas Estuary. Breaks in the pH time series lines represent missing data



value of 471 ± 106 (S.D.) $\mu\text{mol/mol}$ measured in the neighboring Nueces estuary (Walther and Nims 2014). The linear nature of the observed Ba:Ca-salinity relationships was likely due to the high salinity range sampled (>15 ppt). Non-linear

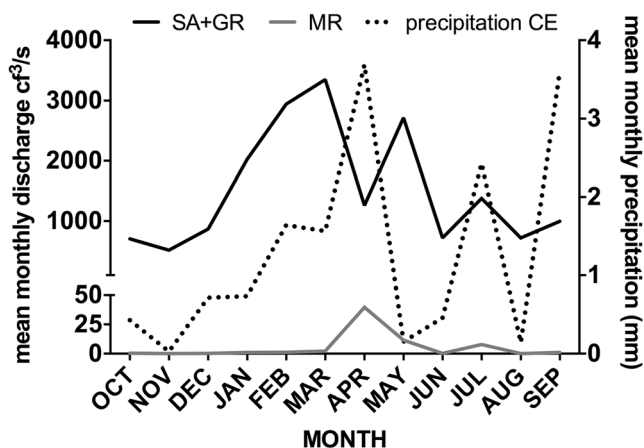
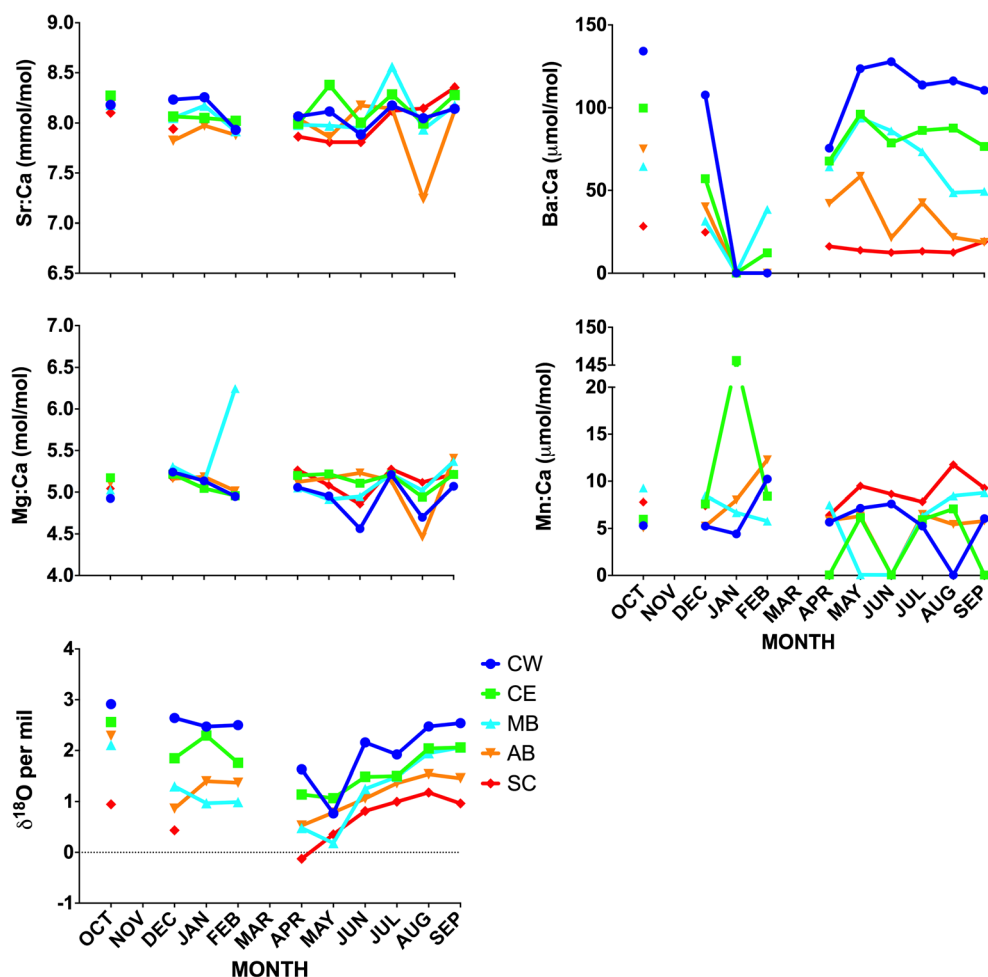


Fig. 5 Mean monthly discharge for the Mission River (MR) at USGS station gauge 8189500 in Refugio, TX and summed discharge (USGS 8188500 + USGS 8176500) of the San Antonio (SA) and Guadalupe Rivers (GR). Daily cumulative precipitation data recorded at the Copano East (CE), the only site with meteorological data

curved behavior would be expected for Ba:Ca at lower salinities, but linear behavior is expected at higher salinities (Coffey et al. 1997; Walther and Nims 2014). If linear mixing of barium at low salinities is assumed, then the effective river end-member (EREM) concentration can be estimated (Coffey et al. 1997; Sinclair and McCulloch 2004). The Ba EREM estimates the total effective flux of Ba from a river including dissolved Ba inputs and the contribution from desorption processes from the suspended particulate matter load (Sinclair and McCulloch 2004) and is useful for making comparisons between rivers. However, interpreting the y-intercept as effective river end-member concentrations may not apply in the Mission-Aransas, where multiple tributaries with distinct Ba end-members all contribute water masses that vary in relative magnitude geographically and temporally. Dorval et al. (2005) reported linear behavior of dissolved barium in the Chesapeake Bay across a salinity gradient (13–27 ppt) similar to our study. In contrast, Hanor and Chan (1977) describe highly non-linear behavior of dissolved Ba due to low-salinity desorption of particulate Ba in the mixing zone of the Mississippi River. Low-salinity peaks in dissolved Ba are commonly reported in estuaries across the world, but the location and magnitude of the peak along the salinity gradient

Fig. 6 Time series of dissolved elemental and isotopic constituents in the Mission-Aransas from October 2011 to September 2012. Different colors represent different sites. Note that sampling was not conducted in November and March (*breaks in line*). Note: break in Y-axis for Mn:Ca. Dotted line in $\delta^{18}\text{O}$ plot indicates expected oceanic $\delta^{18}\text{O}$ value of 0‰

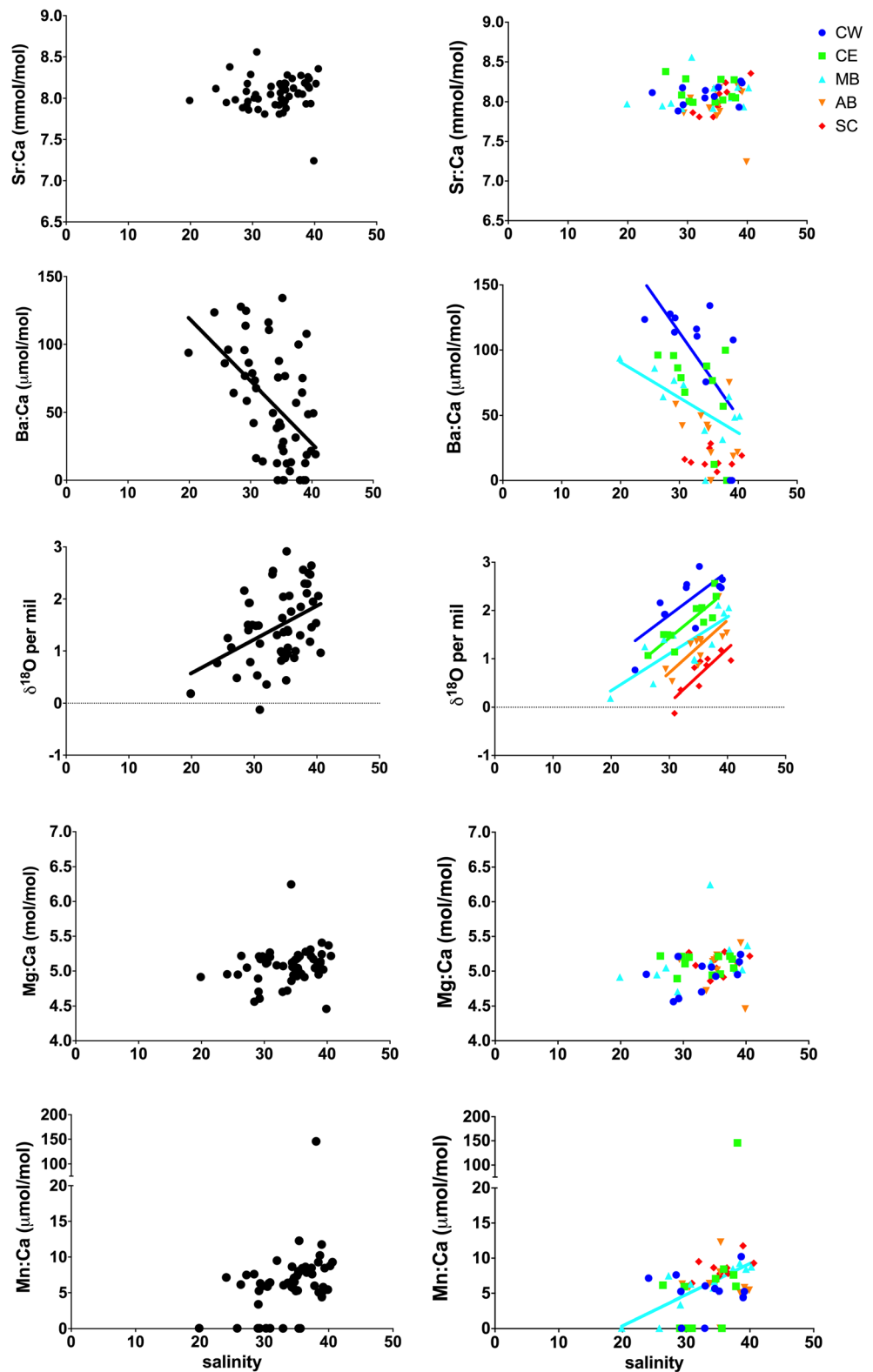


vary depending on estuarine particle dynamics, riverine sediment delivery, and Ba storage/release in salt marshes (Coffey et al. 1997). Barium ions adsorbed to suspended particulate matter (SPM) in freshwater will be exchanged with major cations in seawater, resulting in mid-salinity peaks in dissolved Ba (Hanor and Chan 1977). Barium:Ca displayed consistent linear behavior across the range of salinities (15–43 ppt) we sampled, but non-linear behavior would most likely be detected if lower salinities were sampled (Hanor and Chan 1977; Coffey et al. 1997, Walther and Nims 2014). Novel behavior of dissolved Ba was found in the Coorong Lagoon of Australia, where the Ba-salinity relationship displayed expected negative slopes from salinities of 0 to 37 ppt but switched to unexpected positive slopes from 37 to 120 ppt (Gillanders and Munro 2012). Hypersalinities >42 ppt did not disrupt the dissolved Ba:Ca-salinity relationships in the Laguna Madre; however, Gillanders and Munro (2012) sampled salinities >100 ppt, and these highly concentrated ion concentrations may be required to disrupt expected Ba:Ca-salinity relationships. Additional factors that may disrupt linear Ba-salinity relationships include submarine groundwater discharge (Shaw et al. 1998; Walther and Nims 2014),

dissolution and diffusion from the sediment (Joung and Shiller 2014), and anthropogenic activities (i.e., drilling muds) (Joung and Shiller 2013).

Stable oxygen isotopes were consistently positively related to salinity over both regional and seasonal scales, but at local scales within the Mission-Aransas evaporation-enriched ^{18}O at lower salinities, resulting in a negative linear fit. Several studies have found positive linear relationships between $\delta^{18}\text{O}$ and salinity (Ingram et al. 1996; Cooper et al. 1997). The $\delta^{18}\text{O}$ of estuarine water is both a mixture of groundwater sources and precipitation (Stalker et al. 2009). Evaporative processes can lead to enriched $\delta^{18}\text{O}$ values due to preferential escape of light ^{16}O atoms (Stalker et al. 2009). In the Mission-Aransas, evaporative processes increased $\delta^{18}\text{O}$ values at Copano West and Copano East, the two sites furthest from the ocean, which resulted in the negative relationship between $\delta^{18}\text{O}$ and salinity in Mission-Aransas during July (Stalker et al. 2009). This result contrasts that of Walther and Nims (2014) who found no relationship of $\delta^{18}\text{O}$ to salinity (0–50 ppt) in the Nueces River in neighboring Corpus Christi Bay in 2011, potentially due to evaporative enrichment of ^{18}O atoms during the

Fig. 7 Element-salinity relationships for all Mission-Aransas sites combined (*left column*) and for each site individually (*right column*) throughout the year. Different color lines represent different sites and *plotted lines* display significant linear regressions. *Dotted lines* indicate expected oceanic $\delta^{18}\text{O}$ value of 0‰



drought-dominated period that was sampled. We found a strong relationship between regional evaporation rates and $\delta^{18}\text{O}$, indicating that evaporation increasingly dominates $\delta^{18}\text{O}$ behavior in subtropical estuaries with

decreasing latitude. It is therefore important to consider local evaporative effects that can disrupt predictable relationships of water $\delta^{18}\text{O}$ to salinity in some subtropical systems when choosing reliable salinity proxies.

Table 2 Pearson correlation results between dissolved elements and environmental factors in the Mission-Aransas sampled for 12 months. Significant ($p < 0.05$) correlations using Bonferroni probabilities are indicated in bold. The Ship Channel site and pH were excluded due to missing data

Element	Salinity	Temperature	DO	Chl <i>a</i>
Sr:Ca mmol/mol	-0.06	-0.04	-0.01	0.09
Ba:Ca μ mol/mol	-0.494	0.45	-0.35	-0.03
$\delta^{18}\text{O}$ per mil	0.59	-0.12	-0.06	-0.23
Mg:Ca mol/mol	0.129	-0.196	0.2	0.03
Mn:Ca μ mol/mol	0.19	-0.32	0.18	0.19

On regional and local scales, both Sr:Ca and Mg:Ca exhibited very similar behavior. Neither dissolved constituent varied more than 1 mmol/mol (Sr:Ca) or mol/mol (Mg:Ca) and very similar slopes were detected ranging from 0.028 to 0.038 (Table 1), indicating minimal variation over the salinity ranges sampled. The underlying geology of this region of the Texas coast tends to be primarily carbonates, which are typically high in Sr, Mg, and Ca. Due to the limited range of variation, dissolved concentrations of Sr and Mg may provide limited information as salinity proxies along the Texas coast (Walther and Nims 2014).

The dissolved element ratio which exhibited the highest variability across all spatial and temporal scales was Mn:Ca. The behavior of the redox-sensitive element manganese is controlled mostly by redox potentials, in contrast to the other element examined that tend to vary by salinity. In experimental conditions, changes in pH and physical disturbance of the sediments can influence dissolved Mn release more than changes in dissolved oxygen or salinity (Atkinson et al. 2007). On a coast-wide regional scale, dissolved Mn:Ca was significantly positively related to salinity, although on a local scale, only the Mission-Aransas showed a positive Mn:Ca-salinity relationship. Several other studies have reported non-linear behavior of Mn:Ca across salinity gradients (Dorval et al. 2005; Gillanders and Munro 2012). Additionally, the slope and y -intercept of the Mn:Ca-salinity relationship were highly variable across spatial and temporal scales indicating less reliability as a salinity proxy. However, if the variation in dissolved Mn is influenced by redox potentials and DO levels, then Mn:Ca in calcified structures may provide information on dissolved oxygen exposure histories (Limburg et al. 2011; Mohan et al. 2012; Limburg et al. 2014).

Temporal Patterns

Similar to observed spatial patterns, both Ba:Ca and $\delta^{18}\text{O}$ exhibited consistent temporal patterns over a 12-month sampling schedule. The sampling stations used in Mission-Aransas display distinct distance-to-ocean gradients in

Ba:Ca values, with values decreasing across sites ranking from farthest to closest to the Gulf of Mexico in order Copano West > Copano East > Mesquite Bay > Aransas Bay > Ship Channel. Interestingly, both Ba:Ca and $\delta^{18}\text{O}$ maintained this distinct gradient for every month except two distinct instances. In January, dissolved barium was depleted below detection at all sites, which coincided with lowest annual temperatures. Besides salinity, temperature was the only other environmental factor that was related to Ba:Ca. It is difficult to pinpoint the mechanism for decreased dissolved Ba:Ca in January, but potentially reduced freshwater inputs had influenced Ba:Ca behavior. There was minimal precipitation (<1 mm) and very low river discharge from November through January in the Mission-Aransas. Perhaps, low freshwater inputs did not deliver much SPM to Copano Bay in the winter, resulting in less desorption of barium from SPM due to ion exchange and thus decreased dissolved pools of barium (Coffey et al. 1997). Although we detected high variation in Ba on monthly time scales, Elsdon and Gillanders (2006) found large variation in dissolved Ba at small temporal scales of days and weeks in three different Australian estuaries. Stecher and Kogut (1999) reported rapid dissolved Ba removal in the Delaware estuary that was associated with the end of the spring bloom and barite precipitation and depletion of the dissolved Ba pool. Chl *a* data from the Mission-Aransas exhibits increases in April at all sites in response to the inflow event but not in January. Thus, dissolved Ba depletion due to phytoplankton-associated barite precipitation does not seem to account for the decrease in Ba:Ca in January at all Mission-Aransas sites.

Similar to Ba:Ca, stable oxygen isotopes did show distinct spatial separation between sites throughout the year ranking from most enriched to least enriched Copano West > Copano East > Mesquite Bay > Aransas Bay > Ship Channel. Values of $\delta^{18}\text{O}$ did converge in May in response to the elevated spring discharge, but sites returned to unique values the next month in June. In contrast to the seasonal and spatial variability of Ba:Ca and $\delta^{18}\text{O}$, Sr:Ca and Mg:Ca exhibited limited variation across all months at each site. As mentioned above, these patterns may be due to the limited range of salinities sampled (20–39 ppt) in the Mission-Aransas for the sampled year. Curvilinear mixing curves of both Sr:Ca and Mg:Ca have been reported in systems with salinities <20, with both elemental ratios decreasing at low salinities (Walther and Nims 2014; Gillanders and Munro 2012; Mohan et al. 2012). Manganese:Ca also exhibited limited seasonal variation with values <10 μ mol/mol, except for one large spike in January only at Copano East when dissolved Mn:Ca reached 145 μ mol/mol. A potential explanation for the spike may have been a sedimentary disturbance, which could have delivered reduced Mn^{2+}

from the sediments into the water column. Dissolved oxygen levels were above 5 mg/l throughout the year, indicating that a hypoxic event was not the source of elevated Mn at Copano East in January. Many other studies have found high spatial (Statham et al. 2005) and temporal (Shiller 1997; Elsdon and Gillanders 2006) variation in dissolved Mn, which is not unexpected since Mn behavior is highly influenced by natural redox cycles and mediated by microbial activities (Thamdrup et al. 1994; Pakhomova et al. 2007; Richard et al. 2013).

Conclusions

We found that dissolved Ba:Ca displays consistent up-estuary to down-estuary concentration gradients in subtropical estuaries in Texas, suggesting Ba:Ca would be reliable for tracking animal movements across the ocean–estuary gradient even during periods of reverse estuary conditions. On seasonal scales, dissolved Ba:Ca decreased sharply in the winter, potentially related to decreased delivery of SPM and decreased ion exchange, depleting dissolved Ba pools. Stable oxygen isotopes displayed positive conservative behavior across regional and temporal scales, but the relationship was reversed in the Mission-Aransas due to local evaporation effects. Although dissolved Sr:Ca and Mg:Ca also exhibited conservative behavior, the minimal variation we detected in these ratios makes them less reliable proxies of salinity in south Texas estuaries. Although $\delta^{18}\text{O}$ values varied positively or negatively with salinity at regional and local scales, these dynamics were strongly driven by the magnitude of evaporative processes in driving local enrichment of $\delta^{18}\text{O}$ values. Together, these results suggest that dissolved Ba:Ca exhibits the most reliable gradient along the estuary–ocean continuum due to mixing between freshwater and marine end-members, and this constituent holds the best promise for reconstructing movements of mobile fauna with calcified hard parts, such as fish otoliths.

Acknowledgments We are much obliged for the assistance of J. Barnes, D. Breecker, J. Banner, and N. Miller at the Jackson School of Geosciences for help with sample analysis and R. Mooney, B. Dean, L. Pollard, and staff at the Texas Parks and Wildlife Department for help with sample collection. Helpful comments were provided by G. Ward, two anonymous reviewers, and editor D. Swaney that considerably improved the manuscript. This work was conducted in part in the Mission-Aransas National Estuarine Research Reserve, part of the National Estuarine Reserve System under an award from the Estuarine Reserves Division, Office of Ocean and Coastal Resource Management, National Ocean Service, and National Oceanic and Atmospheric Administration. Funding during this study was provided by Mission-Aransas National Estuarine Research Reserve GRA to J. Mohan and EPA STAR fellowship to J. Mohan.

References

- Atkinson, C.A., D.F. Jolley, and S.L. Simpson. 2007. Effect of overlying water pH, dissolved oxygen, salinity and sediment disturbances on metal release and sequestration from metal contaminated marine sediments. *Chemosphere* 69: 1428–37. doi:10.1016/j.chemosphere.2007.04.068.
- Benoit, G., S.D. Oktay-Marshall, A. Cantu II, E.M. Hood, C.H. Coleman, M.O. Corapcioglu, and P.H. Santschi. 1994. Partitioning of Cu, Pb, Ag, Zn, Fe, Al, and Mn between filter-retained particles, colloids, and solution in six Texas estuaries. *Marine Chemistry* 45: 307–336.
- Coffey, M., F. Dehairs, O. Collette, G. Luther, T. Church, and T. Jickells. 1997. The behaviour of dissolved barium in estuaries. *Estuarine, Coastal and Shelf Science* 45: 113–121.
- Cooper, L.W., T.E. Whitledge, J.M. Grebmeier, and T. Weingartner. 1997. The nutrient, salinity, and stable oxygen isotope composition of Bering and Chukchi Seas waters in and near the Bering Strait. *Journal of Geophysical Research* 102: 12563–12573.
- Diouf, K., J. Panfili, M. Labonne, C. Aliaume, J. Tomás, and T. Do. Chi. 2006. Effects of salinity on strontium:calcium ratios in the otoliths of the West African black-chinned tilapia *Sarotherodon melanotheron* in a hypersaline estuary. *Environmental Biology of Fishes* 77: 9–20. doi:10.1007/s10641-006-9048-x.
- Dorval, E., C.M. Jones, and R. Hannigan. 2005. Chemistry of surface waters: distinguishing fine-scale differences in sea grass habitats of Chesapeake Bay. *Limnology and Oceanography* 50: 1073–1083. doi:10.4319/lo.2005.50.4.1073.
- Elsdon, T.S., and B.M. Gillanders. 2006. Temporal variability in strontium, calcium, barium, and manganese in estuaries: implications for reconstructing environmental histories of fish from chemicals in calcified structures. *Estuarine, Coastal and Shelf Science* 66: 147–156. doi:10.1016/j.ecss.2005.08.004.
- Flint, R.W. 1985. Long-term estuarine variability and associated biological response. *Estuaries* 8: 158–169.
- Fry, B. 2002. Conservative mixing of stable isotopes across estuarine salinity gradients: a conceptual framework for monitoring watershed influences on downstream fisheries production. *Estuaries* 25: 264–271.
- Gillanders, B.M., and A.R. Munro. 2012. Hypersaline waters pose new challenges for reconstructing environmental histories of fish based on otolith chemistry. *Limnology and Oceanography* 57: 1136–1148. doi:10.4319/lo.2012.57.4.1136.
- Hanor, J.S., and L.H. Chan. 1977. Non-conservative behavior of barium during mixing of Mississippi River and Gulf of Mexico waters. *Earth and Planetary Science Letters* 37: 242–250.
- Ingram, B.L., M.E. Conrad, and J.C. Ingle. 1996. Stable isotope and salinity systematics in estuarine waters and carbonates: San Francisco Bay. *Geochimica et Cosmochimica Acta* 60: 455–467. doi:10.1016/0016-7037(95)00398-3.
- Joung, D., and A.M. Shiller. 2013. Trace element distributions in the water column near the Deepwater Horizon well blowout. *Environmental Science & Technology* 47: 21612168. doi:10.1021/es303167p.
- Joung, D., and A.M. Shiller. 2014. Dissolved barium behavior in Louisiana Shelf waters affected by the Mississippi/Atchafalaya River mixing zone. *Geochimica et Cosmochimica Acta* 141: 301–313.
- Klinkhammer, G.P., and J. McManus. 2001. Dissolved manganese in the Columbia River estuary: production in the water column. *Geochimica et Cosmochimica Acta* 65: 2835–2841.
- Kowalski, N., O. Dellwig, M. Beck, M. Grunwald, C.-D. Dürselen, T.H. Badewien, H.-J. Brumsack, J.E.E. van Beusekom, and M.E. Böttcher. 2012. A comparative study of manganese dynamics in the water column and sediments of intertidal systems of the North

- Sea. *Estuarine, Coastal and Shelf Science* 100: 3–17. doi:10.1016/j.ecss.2011.03.011.
- Kraus, R.T., and D.H. Secor. 2004. Incorporation of strontium into otoliths of an estuarine fish. *Journal of Experimental Marine Biology and Ecology* 302: 85–106. doi:10.1016/j.jembe.2003.10.004.
- Limburg, K.E., C. Olson, Y. Walther, D. Dale, C.P. Slomp, and H. Høie. 2011. Tracking Baltic hypoxia and cod migration over millennia with natural tags. *Proceedings of the National Academy of Sciences of the United States of America* 108: E177–82. doi:10.1073/pnas.1100684108.
- Limburg, K.E., B.D. Walther, Z. Lu, G. Jackman, J. Mohan, Y. Walther, A. Nissling, P.K. Weber, and A.K. Schmitt. 2014. In search of the dead zone: Use of otoliths for tracking fish exposure to hypoxia. *Journal of Marine Systems* 1–12.
- Middelburg, J.J., H. Van Der Comelis, W. Weijden and J.R.W. Woittiez. 1988. Chemical processes affecting the mobility of major, minor, and trace elements during weathering of granitic rocks. *Chemical Geology* 68: 253–273.
- Mohan, J.A., R.A. Rulifson, D. Reide Corbett, and N.M. Halden. 2012. Validation of oligohaline elemental otolith signatures of striped bass by use of in situ caging experiments and water chemistry. *Marine and Coastal Fisheries* 4: 57–70. doi:10.1080/19425120.2012.656533.
- Mooney, R.F., and J.W. McClelland. 2012. Watershed export events and ecosystem responses in the Mission–Aransas National Estuarine Research Reserve, South Texas. *Estuaries and Coasts* 35: 1468–1485. doi:10.1007/s12237-012-9537-4.
- Morris, A.W., R.F.C. Mantoura, A.J. Bale, and R.J.M. Howland. 1978. Very low salinity regions of estuaries: important sites for chemical and biological reactions. *Nature* 274: 678–680.
- Negrel, P., C.J. Allegre, B. Dupre, and E. Lewin. 1993. Erosion sources determined by inversion of major and trace element ratios and strontium isotopic ratios in river water: the Congo Basin case. *Earth and Planetary Science Letters* 120: 59–76.
- Nielsen-Gammon, J., F. Zhang, A. Odins, and B. Myoung. 2005. Extreme rainfall in Texas: patterns and predictability. *Physical Geography* 26: 340–364. doi:10.2747/0272-3646.26.5.340.
- Pakhomova, S.V., P.O.J. Hall, M. Yu. Kononets, A.G. Rozanov, A. Tengberg, and A.V. Vershinin. 2007. Fluxes of iron and manganese across the sediment–water interface under various redox conditions. *Marine Chemistry* 107: 319–331. doi:10.1016/j.marchem.2007.06.001.
- Paucot, H., and R. Wollast. 1997. Transport and transformation of trace metals in the Scheldt estuary. *Marine Chemistry* 58: 229–244. doi:10.1016/S0304-4203(97)00037-6.
- Richard, D., B. Sunby, and A. Mucci. 2013. Kinetics of manganese adsorption, desorption, and oxidation in coastal marine sediments. *Limnology and Oceanography* 58: 987–996.
- Shaw, T.J., W.S. Moore, J. Kloepfer, and M.A. Sochaski. 1998. The flux of barium to the coastal waters of the southeastern USA: the importance of submarine groundwater discharge. *Geochimica et Cosmochimica Acta* 62: 3047–3054.
- Shiller, A.M. 1997. Dissolved trace elements in the Mississippi River: seasonal, interannual, and decadal variability. *Geochimica et Cosmochimica Acta* 61: 4321–4330. doi:10.1016/S0016-7037(97)00245-7.
- Sinclair, D.J., and M.T. McCulloch. 2004. Corals record low mobile barium concentrations in the Burdekin River during the 1974 flood: evidence for limited Ba supply to rivers? *Palaeogeography, Palaeoclimatology, Palaeoecology* 214: 155–174. doi:10.1016/j.palaeo.2004.07.028.
- Stalker, J.C., R.M. Price, and P.K. Swart. 2009. Determining spatial and temporal inputs of freshwater, including submarine groundwater discharge, to a subtropical estuary using geochemical tracers, Biscayne Bay, South Florida. *Estuaries and Coasts* 32: 694–708. doi:10.1007/s12237-009-9155-y.
- Statham, P.J., D.P. Connelly, C.R. German, T. Brand, J.O. Overnell, E. Bulukin, N. Millard, et al. 2005. Spatially complex distribution of dissolved manganese in a fjord as revealed by high-resolution in situ sensing using the autonomous underwater vehicle Autosub. *Environmental Science Technology* 39: 9440–9445.
- Stecher, H.A., and M.B. Kogut. 1999. Rapid barium removal in the Delaware estuary. *Geochimica et Cosmochimica Acta* 63: 1003–1012.
- Thamdrup, B., R.N. Glud, and J.W. Hansen. 1994. Manganese oxidation and in situ manganese fluxes from a coastal sediment. *Geochimica et Cosmochimica Acta* 58: 2563–2570.
- Tolan, J.M. 2007. El Niño–Southern Oscillation impacts translated to the watershed scale: estuarine salinity patterns along the Texas Gulf Coast, 1982 to 2004. *Estuarine, Coastal and Shelf Science* 72: 247–260. doi:10.1016/j.ecss.2006.10.018.
- Trefry, J.H., and B.J. Presley. 1982. Manganese fluxes from Mississippi Delta sediments. *Geochimica et Cosmochimica Acta* 46: 1715–1726.
- Walther, B.D., and M.K. Nims. 2014. Spatiotemporal variation of trace elements and stable isotopes in subtropical estuaries: I. Freshwater endmembers and mixing curves. *Estuaries and Coasts*. doi:10.1007/s12237-014-9881-7.
- Ward, G.H. 2010. *Inflows to San Antonio Bay*. Austin: Center of Research in Water Resources, University of Texas at Austin.
- Wen, L.-s., P. Santschi, G. Gill, and C. Paternostro. 1999. Estuarine trace metal distributions in Galveston Bay: importance of colloidal forms in the speciation of the dissolved phase. *Marine Chemistry* 63: 185–212.
- Zhang, J. 1995. Geochemistry of trace metals from Chinese river/estuary systems: an overview. *Estuarine, Coastal and Shelf Science* 41: 631–658. doi:10.1006/ecss.1995.0082.
- Zwolsman, J.J.G., and G.T.M. van Eck. 1999. Geochemistry of major elements and trace metals in suspended matter of the Scheldt estuary, southwest Netherlands. *Marine Chemistry* 66: 91–111. doi:10.1016/S0304-4203(99)00026-2.